A&A 418, 813–825 (2004)
DOI: 10.1051/0004-6361:20034467

Astronomy & Astrophysics

Evolution of BL Lacertae host galaxies⋆,⋆⋆, ⋆⋆⋆

J. Heidt[1], M. Tröller[1,2], K. Nilsson[3], K. Jäger[4], L. Takalo[3], R. Rekola[3], and A. Sillanpää[3]

[1] Landessternwarte Heidelberg, Königstuhl, 69117 Heidelberg, Germany
[2] Metsähovi Radio Observatory, Metsähovintie 114, 02540 Kylmälä, Finland
[3] Tuorla Observatory, 21500 Piikkiö, Finland
[4] Universitätssternwarte Göttingen, Geismarlandstr. 11, 37083 Göttingen, Germany

Received 7 October 2003 / Accepted 14 January 2004

Abstract. We present and discuss deep, high-resolution I-band images of 24 BL Lac objects between $z = 0.3$ and 1.3 taken with the Nordic Optical Telescope (NOT) and the ESO-NTT and VLT telescopes. In addition, new redshifts for the BL Lac objects PKS 0406+121, PKS 0426–380 and PKS 1519–273 are reported.

In 17/24 (71%) of the BL Lac objects, we detected an underlying nebulosity, in 11/17 for the first time. We assigned the underlying nebulosity to the BL Lac host galaxy in 11 cases spanning the redshift range $z = 0.3-1$. The remaining 6 BL Lac objects have either intervening galaxies (S4 0218+35, PKS 0426–380), no redshift (MH 2133–449) or are probably misidentified (Q 0230+3429, B2 0937+26, MS 2347.4+1924).

Restricting ourselves to the 11 BL Lac objects ($\langle z \rangle = 0.6$), where a core and host galaxy was detected, we find that their host galaxies are luminous ($M_I = -25.2 \pm 0.8$) and large ($r_e = 10.5 \pm 7$ kpc). They are on average about 0.6 mag brighter than BL Lac host galaxies at $z \sim 0.3$ indicative of evolution, whereas their half-light radii are similar.

By combining our data with literature data at low-redshift and applying evolutionary models to them, we show that the properties of the host galaxies of BL Lac objects up to $z \sim 1$ are compatible with passively evolving elliptical galaxies formed at a redshift of $z \sim 2$ (13 Gyrs ago in our adopted cosmology).

Our results, however, are affected by an unavoidable luminosity bias and need to be confirmed. Future prospects are described. If they could be confirmed, host galaxies of low-luminosity radio-loud AGN (BL Lac/FR I) have very similar properties to the hosts of radio-quiet QSOs and high-luminosity radio-loud AGN (radio-loud QSO/FR II) over a wide redshift range. This supports the picture of the "Grand Unification" in which AGN activity is a transient phenomenon in galaxy evolution.

Key words. methods: data analysis – galaxies: active – galaxies: BL Lacertae objects: general – galaxies: evolution – galaxies: fundamental parameters – galaxies: photometry

1. Introduction

The similarity of the star formation densities of star-forming galaxies (see e.g. Giavalisco 2002) and the UV luminosity densities of QSOs (see e.g. Wolf et al. 2003) as a function of cosmic epoch point to a close connection between the formation and evolution of galaxies and supermassive Black Holes (presumably the powerhouses of an AGN). This is supported by a) the detection of supermassive Black Holes in the centers of many local massive, inactive, bulge-dominated galaxies (see Kormendy 2003 for the latest compilation) and b) by a strong correlation between the mass of the Black Hole and the mass as well as the velocity dispersion of the harboring inactive galaxy (Magorrian et al. 1998; Ferrarese & Merritt 2000; Gebhardt et al. 2000). Clearly, if the formation and evolution of galaxies and QSOs is closely connected one would also expect the host galaxies of QSOs to be practically indistinguishable from normal inactive galaxies.

Indeed, the host galaxies of radio-quiet quasars (RQQ), radio-loud quasars (RLQ) and of FR II radio galaxies at low-redshift ($z < 0.5$), are luminous and large bulge-dominated galaxies (e.g. Dunlop et al. 2003; Falomo et al. 2003; Floyd et al. 2004; Pagani et al. 2003), follow well the Kormendy (1977) relation for inactive galaxies by Hamabe & Kormendy (1987) and show the same correlation between the

Send offprint requests to: J. Heidt,
e-mail: jheidt@lsw.uni-heidelberg.de

⋆ Based on observations collected with the VLT−UT1 on Cerro Paranal (Chile), the NTT on La Silla (Chile) operated by the European Southern Observatory in the course of the observing proposals 64.P-0230 and 66.B-0125.

⋆⋆ Based on observations made with the Nordic Optical Telescope, operated on the island of La Palma jointly by Denmark, Finland, Iceland, Norway, and Sweden, in the Spanish Observatorio del Roque de los Muchachos of the Instituto de Astrofisica de Canarias.

⋆⋆⋆ Appendix A is only available in electronic form at http://www.edpsciences.org

mass of the Black Hole and their luminosity as their inactive counterparts (McLure & Dunlop 2002).

At higher redshift ($z = 0.8-2$) their host galaxies are more luminous, have similar sizes and show a similar Kormendy relation (if corrected for passive evolution) (e.g. McLure & Dunlop 2000; Falomo et al. 2001; Kukula et al. 2001; Zirm et al. 2003). There possibly exist differences between the hosts of RLQ and RQQ at $z \sim 2$ (e.g. Lowenthal et al. 1995; Hutchings 1995; Kukula et al. 2001).

In general, there is common agreement that the host galaxies of RQQ, RLQ and FR II radio galaxies are indistinguishable from normal massive bulge-dominated galaxies with formation epochs of $z \geq 2-4$ followed by passive evolution thereafter.

The picture is not that clear for the low-luminosity radio-loud AGN (FR I radio galaxies and BL Lac objects). FR I radio galaxies are hard to detect at $z > 0.2$ (Wall & Peacock 1985; Morganti et al. 1995). Even in the FIRST Survey (Becker et al. 1995) most FR I are at $z < 0.2$ with only a few detected up to $z = 0.5$ (Magliocchetti et al. 2000, 2002). Therefore, any morphological information for FR I host galaxies is restricted to local samples.

Govoni et al. (2000) and Bettoni et al. (2001, 2003) found that FR I host galaxies at $z < 0.1$ are luminous, large, bulge-dominated galaxies with their Kormendy relation and Fundamental Plane (Dressler et al. 1987; Djorgovski & Davis 1987) fitting well with the ones obtained for non-active elliptical galaxies.

The best possibility to study host galaxies of low-luminosity radio-loud AGN over a wide redshift range and therefore to investigate, if they follow the same trends found for high-luminosity radio-loud AGN is to use BL Lac objects. Within the Unified Scheme for radio-loud AGN, they are FR I radio galaxies, whose beamed, relativistic jet is seen closely aligned along the line-of-sight to the observer (Urry & Padovani 1995). Hence they can be detected at high redshifts. Their major characteristics are non-thermal emission from radio up to X-ray frequencies (in some cases even up to the γ-ray regime), mostly weak or even absent emission lines in their optical spectra and rapid and strong variability in the total and polarized light.

Due to their extreme properties it is hard to determine their redshifts. For example, the latest compilation of BL Lac objects in the Quasar catalog of Véron-Cetty & Véron (11. edition, 2003) contains ~880 BL Lac objects, but redshifts (or upper limits) are given for ~50% only. Moreover, only about 70 BL Lac objects with $z > 0.5$ from a wide variety of studies are listed (about 35 were known during the time when the observations presented here were conducted), and some of the redshifts are wrong (e.g. PKS 0406+121, see Appendix A). Unfortunately, it is impossible at present to construct a well defined sample of high-redshift BL Lacs to study evolutionary effects.

In the last decade, the host galaxy has been studied in ~150 BL Lac objects with the HST and from ground (e.g. Abraham et al. 1991 (A91); Stickel et al. 1993 (S93); Falomo 1996; Wurtz et al. 1996 (W96); Kotilainen et al. 1998; Wright et al. 1998; Falomo & Kotilainen 1999 (FK99); Heidt et al. 1999a; Urry et al. 1999, 2000 (U00); Scarpa et al. 2000a (S00), 2000b; Pursimo et al. 2002 (P02); Nilsson et al. 2003 (N03); Cheung et al. 2003). The general census is that BL Lac host galaxies are luminous, large elliptical galaxies ($M_R \sim -23.9$, $r_e \sim 10$ kpc), which follow well the Kormendy relation. Their properties are very similar to those of luminous, inactive, local elliptical galaxies.

Contrary to the findings for RQQ, RLQ and FR II radio galaxies, the results cited above were almost exclusively obtained from observations of low-redshift ($z < 0.5$) BL Lac host galaxies. In only 8 BL Lac objects between $0.5 < z < 0.67$ a host galaxy could be detected until now. This is mainly due to the sample selection, the filter used for the observations (see next section) and/or the depth (especially for the HST Snap-survey by S00) or resolution of the images. Clearly, this is not sufficient to study evolutionary effects as has been possible for the RLQ and FR II radio galaxies at least up to $z \sim 1$.

This is further complicated by the fact that BL Lacs at high redshifts are potential candidates for being microlensed objects (background QSOs), whose light from the jet is enhanced with respect to the broad-line region (hiding the line emission in the spectrum). Although there is currently only one clear example of a lensed BL Lac known, (B2 0218+35.7, Patnaik et al. 1993), several more candidates exist (e.g. Heidt et al. 1999b; Scarpa et al. 1999; Heidt et al. 2003b).

In order to increase the number of known BL Lac host galaxies at redshifts $z > 0.5$ and in order to search for any cosmological evolution among those galaxies, we carried out an extensive imaging program using the ESO-NTT, ESO-VLT and NOT telescopes. The results are presented and discussed in the present paper, which is organized as follows: in Sect. 2 we describe the observations and the data reduction followed by the description of the analysis including error estimates and determination of upper limits for non-detected hosts in Sect. 3. In Sect. 4 we describe the global properties of our sample, while we form a core sample and discuss its properties in Sect. 5. Finally, we summarize in Sect. 6. Notes on individual sources and new redshifts for 3 BL Lac objects can be found in the Appendix A.

To facilitate comparison with other studies, $H_0 = 50$ km s^{-1} Mpc^{-1} and $q_0 = 0$ is assumed.

2. Observations and data reduction

2.1. Imaging

Deep, high-resolution images of 24 BL Lac objects in the redshift range $z = 0.3-1.3$ have been taken with SUSI2 at the ESO-NTT on La Silla, Chile, with FORS1 at the ESO-VLT (UT1) on Cerro Paranal, Chile, and with the StanCam at the Nordic Optical Telescope (NOT) on La Palma, Canary Islands. The observations at the NTT were taken in service mode on the night October, 7/8 1999, in visitor mode at the NOT from January 23–27, 2001 and at the VLT during periods of non-observability of the FORS Deep Field project[1] between August 13–17, 1999. In Table 1 the instrumental setup at the individual telescopes is listed.

[1] See Heidt et al. (2003a) for details on the FORS Deep Field project.

Table 1. Instrumental setup for the observations.

Tel./Instr.	CCD	RON	Gain	Scale	FOV
		e^-	e^-/ADU	″/pix	′
NOT/StanCam	1k × 1k	6.50	1.68	0.176	3.0 × 3.0
VLT/FORS1	2k × 2k	5.95	3.17	0.200	6.8 × 6.8
NTT/SUSI2	1k × 2k	4.90	2.25	0.162	2.7 × 5.5

The observations with the StanCam and FORS1 were done in standard resolution mode, whereas the observations with SUSI2 were carried out by binning the CCD by a factor of 2. Except for PKS 1349–439 and MH 2133–449, which were observed with a *R*-filter, we used a *I*-filter throughout the observations. This has the advantage that we sample the spectrum redwards of the 4000 Å break of an elliptical galaxy up to redshifts of $z \sim 1$ thus increasing the chance to detect the host galaxy (note, that the widely used *R*-filter samples the spectrum redwards of the 4000 Å up to $z \sim 0.65$ only). Since the number of BL Lac objects at redshifts larger than $z > 0.5$ is still limited and hence no well defined sample of high redshift BL Lac objects exists, the objects were chosen by observability only.

Each BL Lac was observed between 15 and 180 min in total, depending on the redshift and telescope. In all cases several sufficiently short images to avoid saturation of the BL Lac nucleus were taken. In order to use the frames for fringe correction and superflat purposes, the images were jittered. We typically used a random walk jitter pattern within a rectangular box of 30″ border length centered on the central position. Whereas the observations at the VLT were partly be carried out during periods of non-photometric observing conditions, the data taken at the NOT and NTT where always acquired during photometric nights. During each of the individual nights standard stars from Landolt (1992) were observed to set the zero point.

The individual images were first corrected for bias and then for pixel-to-pixel variations. For the latter we used twilight flatfields. A superflat was created out of the bias-subtracted and flatfielded images to correct for large-scale gradients. To remove the fringes on the NOT and NTT-images a scaled fringe template derived from *I*-band images taken during the individual nights was subtracted. No fringe correction was necessary for the observations taken with the VLT. Finally, the images were cleaned of cosmic ray hits, aligned and summed. The full data set is presented in Table 2.

2.2. Spectroscopy

Low-resolution spectra of four BL Lac objects of our sample were recorded on various occasions with FORS1/2 at the VLT. They were observed because no redshift has yet been determined for them (PKS 1519–273, MH 2133–449) or because we could find a galaxy projected onto the BL Lac nucleus, which was too bright to be at the given redshift (PKS 0406+121) or its upper limit to its redshift (PKS 0426–380).

In all cases we used the grism 150I, which gave us a spectral scale of ∼5.5 Å/pixel for PKS 0426–380 and PKS 1519–273 (observed in September 2001 and 1999, respectively) and ∼6.9 Å/pixel for PKS 0406+121 and MH 2133–449 (observed with the new CCD at FORS2 in August 2003). The slit width was set to 1″. The wavelength range covered was ∼4000–10 000 Å. At the end of each of the nights, spectrophotometric standards from Oke (1990) were observed.

The data reduction of the individual spectra (bias subtraction, flatfielding, cosmic ray removal, sky subtraction, wavelength calibration, etc.) was performed using standard MIDAS routines. The individual spectra were smoothed using a running mean with a width of 3 pixels. The *FWHM* spectral resolution measured from strong night sky emission lines is ∼25 Å.

3. Analysis

3.1. Fitting procedure

To analyze our images of the BL Lac objects, we followed the procedure described in Heidt et al. (1999a) and N03. A 2-dimensional model is fitted to the observed image via an iterative χ^2-minimization using the Levenberg-Marquardt technique. Three different models were fitted. One representing a pure AGN (scaled PSF), one representing an AGN + bulge (scaled PSF + convolved de Vaucouleurs model) and one representing an AGN + disk (scaled PSF + convolved disk model). The core is parameterized by its position (x, y) and magnitude m_c, whereas the host galaxy is parameterized by its position (x, y), its total brightness m_g, effective radius r_e, ellipticity ϵ, position angle PA and the shape parameter β (0.25 for de Vaucouleurs, 1 for Disk). Three different sets with the three different models were fitted. In the first set we did not allow for an offset between the AGN and the putative galaxy, ϵ and PA were set to zero. In the second set we repeated the fits with varying ϵ and PA for the well resolved host galaxies. In the last set involving all objects again, we allowed for an offset between the AGN and the putative galaxy, but set ϵ = PA = 0. The latter is especially useful to search for galaxies along the line of sight projected onto the BL Lac, which might influence the intrinsic properties of the BL Lac objects by means of gravitational microlensing. Obviously, the centers of the galaxies must not necessarily coincide with the centers of the BL Lac objects in that case.

Since our aim was to resolve host galaxies of BL Lac objects at high redshift, great care had to be taken to use a representative PSF. In most cases we were able to use a combination of several (typically 3–5) non-saturated stars of at least a similar brightness as the BL Lac. In those cases, where no sufficiently bright unsaturated stars could be used, the PSF was extracted using a combination of saturated stars (that were used for the outer part) and non-saturated stars (that were used for the central part). SUSI2 consists of a mosaic of 2 CCDs. Here we used only stars present at the CCD, where the BL Lac was located.

Prior to fitting, we masked out carefully all regions affected by nearby companion objects. In five cases (PKS 0057–338, Q 0230+3429, PKS 0823+033, PKS 1519–273, PKS 2029+121)

Table 2. Observing log of the sample.

Object	α(2000)	δ(2000)	z	*FWHM* [″]	$t_{\rm exp}$ [s]	Tel.	z-ref.
PKS 0057–338	01 00 09	−33 37 32	0.875	0.70	1920	VLT	Perlman et al. (1998)
S4 0218+35	02 21 05	35 56 15	0.96	0.79	11040	NOT	Browne et al. (1993)
Q 0230+3429	02 33 20	34 42 54	0.458	0.76	900	NOT	Moran et al. (1996)
PKS 0406+121	04 09 22	12 17 39	0.504	0.91	5220	NOT	present study
PKS 0426–380	04 28 40	−37 56 19	1.110	0.74	5280	NTT	present study
PKS 0754+100	07 57 06	09 56 34	0.266	0.88	5400	NOT	Carangelo et al. (2003)
PKS 0820+225	08 23 24	22 23 03	0.951	1.00	10370	NOT	Stickel et al. (1993)
PKS 0823+033	08 25 50	03 09 24	0.506	1.07	2700	NOT	Stickel et al. (1993)
RX J0930.9+3933	09 30 56	39 33 33	0.638	0.83	5400	NOT	Nass et al. (1996)
B2 0937+26	09 40 13	26 03 26	0.498	1.33	4500	NOT	Perlman et al.(1998)
TXS 1040+224	10 43 09	24 08 35	0.560	0.98	3600	NOT	White et al. (2000)
1207+39W4	12 10 26	39 29 08	0.615	0.94	5400	NOT	Rector et al. (2000)
Q 1214+1753	12 16 56	17 37 12	0.679	1.07	5400	NOT	Hewett et al. (1995)
1ES 1249+174W	12 51 45	17 11 17	0.644	1.04	6900	NOT	Perlman et al. (1996)
PKS 1349–439	13 52 56	−44 12 41	?	1.05	960	VLT	Véron (1995)
RX J1422.6+5801	14 22 39	58 01 55	0.638	0.98	4500	NOT	Bade et al. (1998)
TXS 1428+370	14 30 40	36 49 03	0.564	1.07	3600	NOT	White et al. (2000)
PKS 1519–273	15 22 37	−27 30 10	1.294	0.80	1920	VLT	present study
OV −236	19 24 51	−29 14 31	0.352	0.70	2160	VLT	Scarpa & Falomo (1997)
PKS 2029+121	20 31 55	12 19 49	1.215	1.00	960	VLT	Stocke & Rector (1997)
PKS 2131–021	21 34 10	−01 53 17	1.285	1.00	960	VLT	Drinkwater et al. (1997)
MH 2133–449	21 36 18	−44 43 50	?	1.00	960	VLT	Hawkins (1991)
PKS 2240–260	22 43 26	−25 44 30	0.774	0.75	3240	NTT	Stickel et al. (1993)
MS 2347.4+1924	23 50 01	19 41 52	0.515	0.97	1200	NTT	Rector et al. (2000)

the BL Lac objects had overlapping sources. Here we used an iterative fitting procedure as described in Heidt et al. (1999a). We first fitted the BL Lac and then fitted the companion object on the BL Lac subtracted image. Then we fitted the BL Lac again on the companion object subtracted image and used the new results again to fit the companion object. This procedure was repeated until the fits did not improve further.

3.2. Upper limits and error simulations

To determine the errors of our fits, we followed the procedure described in N03. For each object we created 50 simulated images that correspond to the best fitting parameters and repeated the fits similarly as for the actual data. We added photon noise, readout noise and background uncertainties, the latter of which were measured from several regions nearby the BL Lac objects, to the simulated images. The most critical step was the treatment of the uncertainty of the PSF, which can vary from field to field depending on the S/N of the PSF and the telescope/instrument used. Although tracking errors or seeing changes can be circumvented by using PSF stars from the same field as the BL Lac observed, aberrations in the imaging system can introduce PSF variations across the field and thus degrade the results (see e.g. Heidt et al. 1999c and discussion in N03).

We described each PSF by a Moffat profile that was convolved with an "aberration PSF". The latter was formed by creating a low-order wavefront aberration image parameterized by defocus and astigmatism terms, and Fourier transformed to obtain the focal plane image (see N03 for details). By running a set of 10 fits on the simulated images with 5–10 different slightly defocussed PSFs and by comparing the residuals to the ones on the actual fits, we determined the most reliable defocusing of the PSF, which had to be introduced. This one was then used for the final set of 50 simulations. The errors given in Table 3 are the standard deviation of the parameters in the simulations. To account for the errors of the photometric calibration, we added in square 0.03 mag to the magnitude errors obtained from the error simulations.

To judge if the host galaxy of a BL Lac object is resolved or not (especially at high redshift) is a tricky issue. For a couple of sources (e.g. PKS 2131–021), the fit did not converge to a meaningful solution (exceedingly small half-light radii or exceedingly faint host galaxies). Those sources were defined as unresolved. For the remaining sources we required $r_{\rm e} > 5\sigma_{r_{\rm e}}$ to define an object as resolved, where $\sigma_{r_{\rm e}}$ comes from the error simulations. Since a simple defocusing of the PSF certainly does not take into account all PSF errors, the errors are probably underestimated. We therefore decided to use this rather strict limit.

We have estimated upper limits for the host galaxy brightness using simulated images for our unresolved sources. The simulated images consisted of a core component with the magnitude determined from the fits with a pure core only, and a host galaxy with effective radius $r_{\rm e}$ = 10 kpc. For PKS 1349–439 we assumed z = 0.7 to convert $r_{\rm e}$(kpc) to $r_{\rm e}(″)$. Using progressively fainter host galaxies we determined the highest host magnitude that allowed us to make a host detection, by again running error simulations and using the resolution criterium defined above.

4. Results

The results of our fits for a core plus elliptical galaxy model without decentering and ϵ = PA = 0 (except for B2 0937+26

Table 3. Results of the host galaxy fitting for the de Vaucouleurs model.

Object	z	A_I	K_I	R^a	$m_{\rm core}$	$M_{\rm core}$	$m_{\rm host}$	$M_{\rm host}$	$r_{\rm e}$ [″]	$r_{\rm e}$ [kpc]	$\mu_{\rm e}$ [mag/sq″]	χ^2	$\frac{\chi^2_{\rm deV.}}{\chi^2_{\rm exp}}$
PKS 0057–338	0.875	0.04	1.22	E+	19.65 ± 0.04	−24.78	19.60 ± 0.05	−26.04	0.34 ± 0.06	3.54 ± 0.21	16.66 ± 0.18	4.97	1.09
S4 0218+35	0.936[b]	0.09	1.50	D	19.42 ± 0.05	−25.25	19.67 ± 0.08	−25.60	0.51 ± 0.03	4.79 ± 0.28	17.76 ± 0.20	2.09	0.77
Q 0230+3429	0.500	0.11	0.45	E+	20.60 ± 0.20	−22.38	15.61 ± 0.06	−27.82	4.91 ± 0.28	39.65 ± 2.26	20.18 ± 0.19	1.16	1.04
PKS 0406+121	0.504	1.09	0.46	N+	19.29 ± 0.04	−24.69	19.91 ± 0.17	−24.53	0.54 ± 0.03	4.38 ± 0.24	18.64 ± 0.29	0.96	0.99
PKS 0426–380	1.111[c]	0.06	0.53	D	16.99 ± 0.04	−28.15	20.25 ± 0.12	−23.50	0.82 ± 0.03	7.01 ± 0.26	20.69 ± 0.20	9.30	0.95
PKS 0754+100	0.266	0.04	0.21	E	15.51 ± 0.03	−25.82	17.76 ± 0.04	−23.78	2.46 ± 0.21	13.45 ± 1.15	21.83 ± 0.27	2.02	1.17
PKS 0820+225	0.951	0.08	1.46	N+	18.52 ± 0.04	−26.19	20.67 ± 0.10	−25.50	0.73 ± 0.05	7.82 ± 0.54	18.93 ± 0.25	1.20	1.00
PKS 0823+033	0.506	0.18	0.46	U	16.01 ± 0.06	−27.07	<16.9	<−26.6				8.23	
RX J0930.9+3933	0.638	0.03	0.66	E+	20.30 ± 0.05	−23.25	18.92 ± 0.04	−25.28	1.50 ± 0.10	13.68 ± 0.91	20.36 ± 0.18	1.10	1.35
B2 0937+26[d]	0.498	0.03	0.45	E+			19.43 ± 0.05	−23.91	0.85 ± 0.13	6.84 ± 1.08	20.23 ± 0.39	1.09	1.06
TXS 1040+244	0.560	0.06	0.53	E+	17.40 ± 0.04	−25.83	18.60 ± 0.06	−25.16	0.80 ± 0.11	6.85 ± 0.94	18.98 ± 0.36	1.84	1.12
1207+39W4	0.615	0.06	0.62	E	18.49 ± 0.03	−24.99	18.92 ± 0.09	−25.17	2.81 ± 0.51	25.18 ± 4.57	21.79 ± 0.49	1.87	1.04
Q 1214+1753	0.679	0.07	0.73	N+	17.13 ± 0.03	−26.62	18.99 ± 0.05	−25.50	1.12 ± 0.22	10.50 ± 2.06	19.57 ± 0.48	1.73	1.01
1ES 1249+174W	0.644	0.04	0.67	U	17.96 ± 0.03	−25.62	<19.1	<−25.2				2.18	
PKS 1349–439[e]	?	0.15		U	17.64 ± 0.04	−26.28	<18.7					1.58	
RX J1422.6+5801	0.638	0.02	0.66	N+	17.60 ± 0.03	−25.94	18.86 ± 0.08	−25.33	2.26 ± 0.43	20.60 ± 3.92	21.20 ± 0.49	1.62	1.00
TXS 1428+370	0.564	0.02	0.54	E+	21.36 ± 0.60	−21.85	18.91 ± 0.05	−24.83	0.38 ± 0.04	3.27 ± 0.34	17.70 ± 0.28	1.15	1.07
PKS 1519–273	1.294	0.56	2.58	U	17.88 ± 0.04	−28.21	<18.1	<−30.6				2.64	
OV −236	0.352	0.30	0.29	E	17.02 ± 0.03	−25.25	18.31 ± 0.03	−24.25	1.65 ± 0.13	10.86 ± 0.86	20.89 ± 0.20	10.06	1.36
PKS 2029+121	1.215	0.19	2.28	U	18.33 ± 0.04	−27.20	<19.9	<−27.9				10.29	
PKS 2131–021	1.285	0.13	2.24	U	18.64 ± 0.04	−27.00	<19.9	<−28.3				1.69	
MH 2133–449[e]	?	0.05		N+	18.86 ± 0.03		21.28 ± 0.09		3.73 ± 0.31			1.65	0.99
PKS 2240–260	0.774	0.05	0.94	U	16.00 ± 0.04	−28.09	<17.7	<−27.3				4.98	
MS 2347.4+1924[f]	0.515	0.32	0.47	D			18.85 ± 0.04	−24.89	0.53 ± 0.08	4.36 ± 0.66	18.27 ± 0.37	1.37	0.93

[a] Code for galaxy detection and morphology class: U = unresolved, E = elliptical, D = disk, N = resolved, but unclassified, + new detection.
[b] Grav. lensed BL Lac. $z = 0.96$ used for the core, $z = 0.685$ used for the lensing galaxy.
[c] $z = 1.111$ used for the core, $z = 0.559$ used for the intervening galaxy. See subsection A for details.
[d] Results given for $\epsilon = 0.28$, PA = 30°. See subsection A for details.
[e] Observations taken through Cousins *R*-filter. Extinction and K-correction for corresponding filter used.
[f] Results given for $\epsilon = 0.44$, PA = 65°. See subsection A for details.

and MS 2347.4+1924, see below) are presented in Table 3. For all objects we list the redshift, the interstellar extinction from NED, the K-corrections for elliptical galaxies from Fukugita et al. (1995), a code for galaxy detection and morphology, the apparent and absolute magnitudes of the core and the galaxy as well as the half-light radii of the galaxies in arcsec and kpc and the surface brightness μ_e at r_e. To derive the absolute magnitudes for the hosts, extinction and K-correction was applied, whereas the absolute magnitudes derived for the AGN were extinction corrected but not K-corrected (we assumed a power-law spectrum of the form $I_\nu \propto \nu^{-1}$). The surface brightness μ_e at r_e was corrected for galactic extinction, cosmological dimming and it was K-corrected. The last two columns give the χ^2 for the fit and the χ^2-ratio between the fit with a de Vaucouleurs+core and a disk+core model. The radial profiles for the objects, where a galaxy was detected, are presented in Fig. 1. To allow the reader to assess the quality of the fits, we show in Fig. 2 thumbnail images of the BL Lacs and the best-fit model subtracted images for the fits with a pure core and core+elliptical galaxy. Notes on individual sources can be found in the Appendix A.

According to our fits and the error simulations, we were able to detect a galaxy in 17/24 (71%) BL Lac objects. In 9/17 resolved galaxies an elliptical + core model is slightly preferred over a disk+core model to describe the light distribution of the objects ($\chi^2_{\rm exp}/\chi^2_{\rm deV.} \geq 1.04$). For 5/17 objects no model is preferred over the other ($\chi^2_{\rm exp}/\chi^2_{\rm deV.} = 1.0 \pm 0.01$), while for 3/17 a disk+core model apparently gave a slightly better fit ($\chi^2_{\rm exp}/\chi^2_{\rm deV.} \leq 0.95$). The latter are B2 0218+35, PKS 0426–380 and MS 2347.4+1924 and are discussed in detail in the Appendix A.

Except for B2 0937+26 and MS 2347.4+1924, the analysis with varying ϵ and PA did not result in significantly better fits to the objects. We could not detect a core in these two sources for a bulge+core fit and faint cores when using a disk+core model. The results given in Table 3 for these objects are determined with varying ϵ and PA.

Five out of the 7 remaining sources are clearly unresolved (exceedingly small half-light radii or exceedingly faint host galaxies). The two other sources (PKS 0823+033 and 1ES 1249+174W) have formally better χ^2 values for a core+galaxy fit as for the pure core fit, but they did not meet our resolution criteria according to our error simulations.

Except for the 3 unusual sources (S4 0218+35, lensed BL Lac, PKS 0426–380, intervening galaxy, MS 2347.4+1934, no core detected) for none of the remaining objects in our sample a disk+core fit is clearly preferred over a bulge+disk fit. Similar results have been obtained by FK99, S00 and N03. In the following we assume that the host galaxies of our high-redshift BL Lacs are elliptical galaxies.

5. Discussion

5.1. The core sample

We detected in 17/24 sources (71%) an underlying nebulosity. Neglecting uncertain sources (see below), we are confident that we were able to resolve the host galaxy in 11/24 (46%) of our BL Lac objects. This is most likely due to the choice of the filter used (*I*-band contrary to the other studies, which used almost exclusively a *R*-filter), the long integration times in combination with mostly subarcsecond seeing conditions and the choice of objects with respect to previous studies. E.g. W96 reported marginal detections of the host galaxy for all 6 of their BL Lacs between $z = 0.5$–0.65 (the sample was restricted to $z < 0.65$), whereas in the sample of 52 X-ray selected BL Lac objects studied by FK99 only three sources at $z > 0.5$ were included (all resolved). In the HST-snap survey of 110 BL Lacs (S00) in 6/22 BL Lac objects at $z > 0.5$ a host galaxy was detected, P02 could detect a host galaxy in only 2/12 $z > 0.5$ sources from the 1 Jy sample of BL Lacs. Finally, N03 detected a host in 4/7 BL Lacs at $z > 0.5$ among the 100 BL Lac objects from the ROSAT-Green Bank sample of intermediate BL Lac objects studied. The latter included both X-ray-selected (XBL) and radio-selected (RBL) BL Lacs.

The only study in *I*-band was carried out by Urry et al. (1999), where they were able to resolve a host galaxy for 3 out of 4 $z > 0.5$ BL Lacs. In total, the host galaxy properties could be derived for only 8 $z > 0.5$ sources in the studies of W96, FK99, Urry et al. (1999), S00, P02 and N03.

Two out of the 7 sources with non-detected hosts (PKS 0823+033 and 1ES 1249+174W) had formally a better fit for a core+bulge model, but did not meet our resolution criteria, while 4/7 unresolved sources are at the highest or unknown redshift (PKS 1349–439, PKS 1519–272, PKS 2029+121 and PKS 2131–021). In addition, 3/7 objects had nearby, partly overlapping companion objects (PKS 0823+033, PKS 1519–273 and PKS 2029+121). For none of our 7 unresolved sources a clear detection of its host galaxy was reported in earlier studies.

According to Ostriker & Vietri (1985), some BL Lac objects may be actually background QSOs, whose continuum emission is enhanced by stars in a foreground galaxy by gravitational microlensing relative to the emission of their broad-line region. Naturally, BL Lac objects at higher redshift are such potential candidates. Stocke & Rector (1997) examined the excess of Mg II absorbers in the spectra of BL Lac objects and concluded that microlensing can explain the presence of the Mg II absorbers and the very featureless BL Lac spectra. However, except for the only confirmed lensed BL Lac S4 0218+35 (Patnaik et al. 1993) and a few more conspicuous cases (Scarpa et al. 1999), the evidence is weak (see Heidt et al. 2003b; Heidt 1999b and references therein). Our observations confirm this. According to our fits with decentering, all host galaxies are centered within 0.″03 onto the BL Lac. The only exception is PKS 0426–380, where we detected a galaxy with decentering of ∼0.″17 with respect to the BL Lac and which has two absorbers along the line of sight. Unfortunately, PKS 0426–380 is a southern object and therefore not included in long-term variability monitoring programs, which allow to test the microlensing hypothesis for this object.

In order to study evolutionary effects of the host galaxies and to compare our results to those obtained by others, we define a "core" sample of 11 BL Lac objects devoid of "misidentified" host galaxies or other spurious effects. The 6 sources which we exclude are S4 0218+35 (lensed

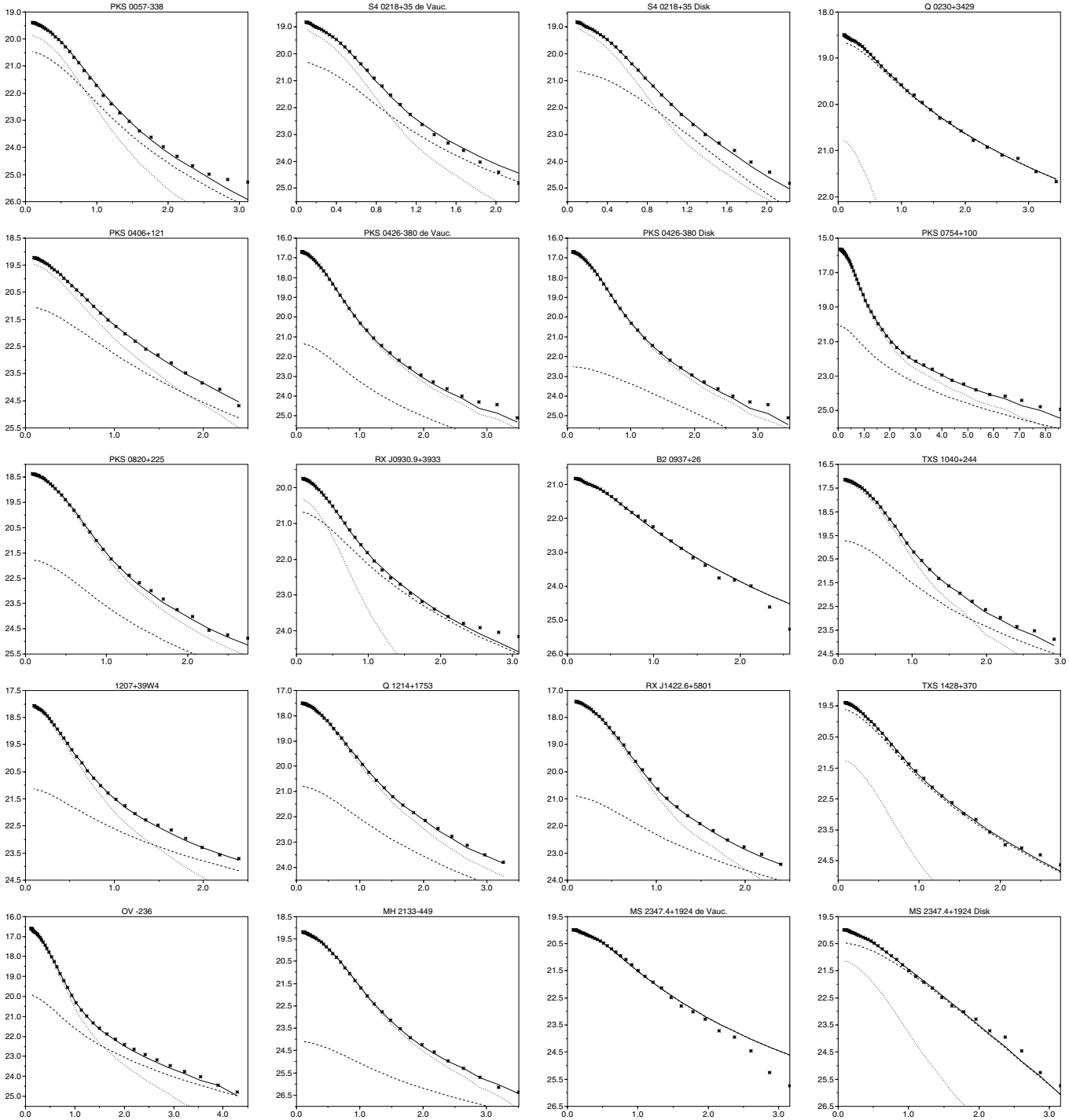

Fig. 1. Radial profiles of our objects, where a galaxy has been detected. Asterisks mark the observed points, the dashed line the host galaxy model, the dotted line the core model and the solid line the sum of host + core model. For S4 0218+35, PKS 0426–380 and MS 2347.4+1924, the radial profiles are shown for an elliptical- and a disk-type host galaxy model. The x-axis shows the distance from the nucleus in arcsec. Apart from MH 2133–449 (R-band), the y-axis gives the I-band surface brightness in mag arcsec^{-2}.

BL Lac), Q 0230+3429 (BL Lac classification uncertain, galaxy found most likely at different z), PKS 0426–380 (galaxy detected most likely an absorber along the line-of-sight), MH 2133–449 (unknown redshift) as well as B2 0937+26 and MS 2347.4+1924 (no core detected). Our core sample spans the range $z = 0.3{-}1$ ($\langle z \rangle = 0.6 \pm 0.2$) with 9 sources at $z > 0.5$, efficiently doubling the number of detected BL Lac hosts at $z > 0.5$. The BL Lac with the highest redshift, where the host galaxy was detected, is PKS 0820+225 at $z = 0.951$.

The median absolute magnitude of the host galaxies of our core sample is $\langle M_I \text{ (host)} \rangle = -25.2 \pm 0.7$. Assuming a color of $R - I = 0.7$ for local elliptical galaxies (Fukugita et al. 1995) we derive $\langle M_R \text{ (host)} \rangle = -24.5$. This value is about 0.6 mag brighter as has been determined for lower-redshift ($\langle z \rangle \sim 0.25$)

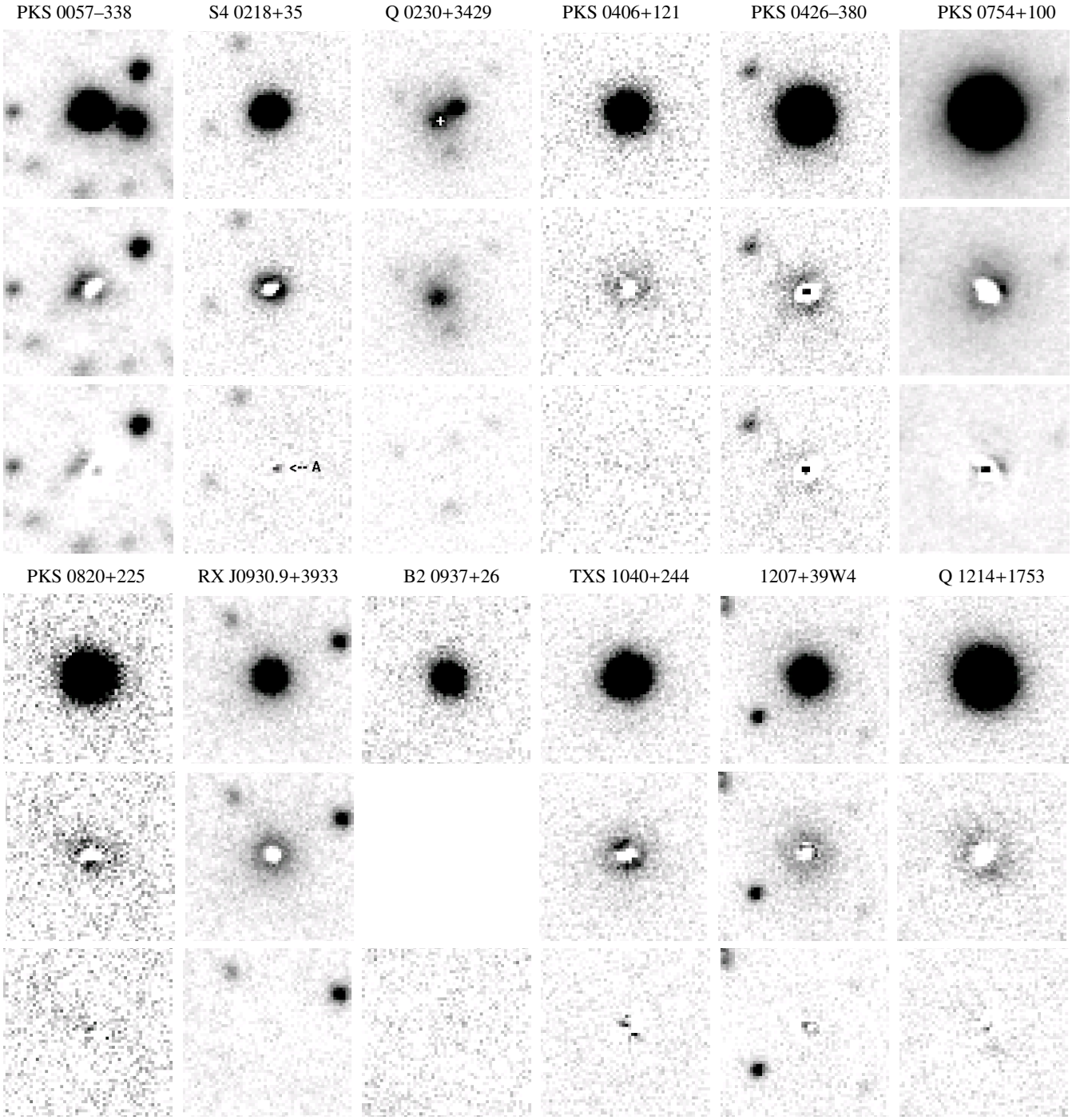

Fig. 2. Thumbnail images of the 17 BL Lac objects, where we detected an underlying nebulosity. For each object we show (from top to bottom) the BL Lac, the image after subtraction of the best-fit core model and the image after subtraction of the best-fit core+elliptical galaxy model. Note that a white spot in the center row (best-fit core model) comes from an oversubtracted PSF in the center of the BL Lac due to the χ^2-minimization. This is indicative of light from a galaxy, since its light distribution is shallower. For PKS 0057–338 we show the best fit after subtraction of the companion galaxy to the W. The BL Lac component A in the lensed BL Lac S4 0218+35 is indicated. For Q 0230+3429, we show the image after subtraction of the unresolved object 1.″2 to the NW and the best-fit galaxy model without core. The position of the radio source is marked with a cross. For B2 0937+26 and MS 2347.4+1924 no core was detected. Here we show the image after subtraction of the best-fit galaxy model with variable ϵ and PA. FOV is 10″on each side, N is up, E to the left.

samples by W96, FK99, S00, P02 and N03 and indicates an evolution of BL Lac host galaxies from high to low redshifts. However, as can be seen from Fig. 3a, we are subject to a luminosity bias (at higher redshift only the brighter hosts can be detected), so this conclusion should be treated with caution. The median absolute magnitude of the AGN in our core sample is $\langle M_I \text{ (core)} \rangle = -25.3 \pm 1.4$ (-25.9 ± 1.6 including the 6 unresolved objects with known redshift and PKS 0426–380).

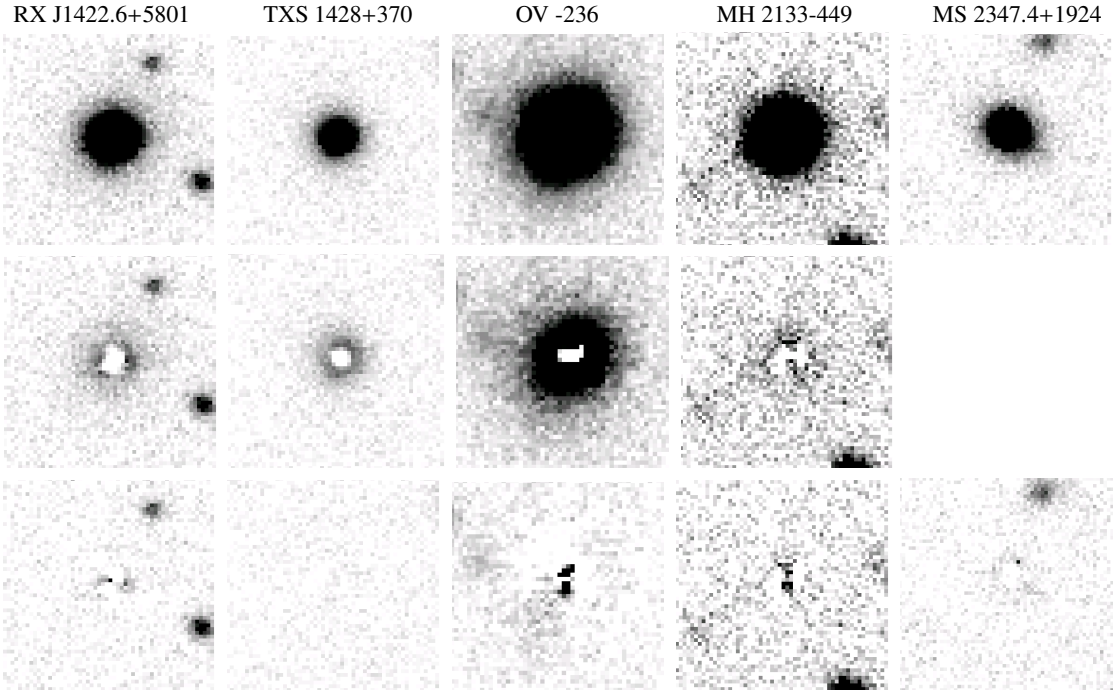

Fig. 2. Continued.

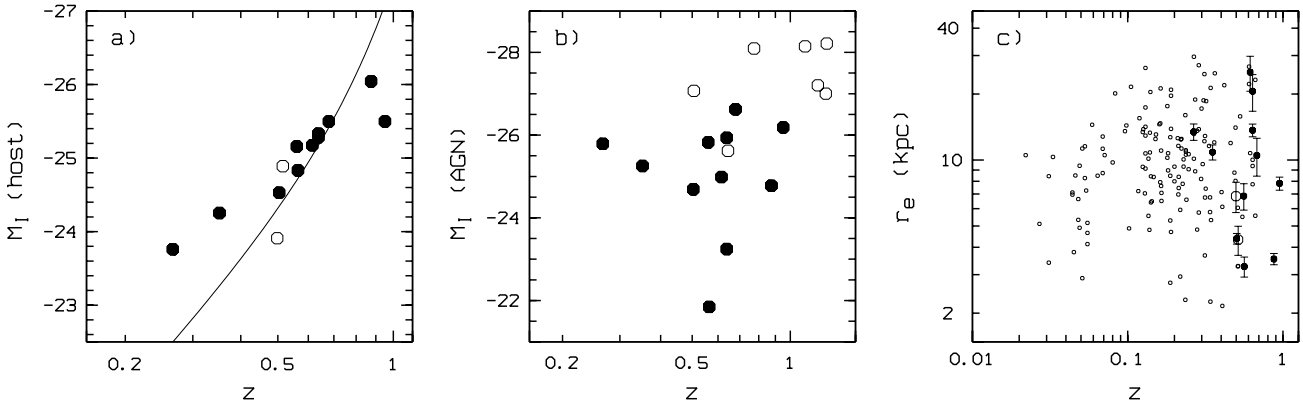

Fig. 3. a) Absolute host galaxy *I* magnitudes of the core sample (black boxes) versus redshift. The line gives the absolute magnitude of an object with $I = 19$, with K-correction, but no evolution. The two sources without core (B2 0937+26 and MS 2347.4+1924) are also included (open circles). **b)** Absolute AGN *I* magnitude of the core sample (black boxes) and the unresolved sources with known redshift + PKS 0426–380 (open boxes) versus redshift. **c)** Host galaxy half-light radius versus redshift for the core sample (black boxes), the two sources without core (B2 0937+26 and MS 2347.4+1924, open circles) compared to the HST-Snap, XBL and RGB-samples (S00, FK99, N03, small boxes). The measured values are roughly constant from $z = 0.1$ up to $z = 1$.

Since the objects have been selected from flux-limited samples, a selection effect is apparent again (Fig. 3b).

The median scale length of the hosts in our core sample is $\langle r_e \rangle = 10.5 \pm 7$ kpc. Similar values have been derived by W96, FK99, S00 and N03 for ($\langle z \rangle \sim 0.25$) BL Lacs and by Govoni et al. (2000) for $z < 0.1$ FR IIs. Curiously, the FR Is studied from ground by Govoni et al. (2000) at $z < 0.1$ seem to have somewhat larger half-light radii contrary to what has been found by U00 for $z < 0.1$ BL Lacs with HST. This may be due to the limited field of view by the WFPC2 detector used by S00 (see discussion in Barth et al. 2003). Nevertheless, our data confirm that there is no correlation of the half-light radii with redshift up to the highest redshifts probed (Fig. 3c). Noticeably, no correlation of the half-light radii with redshift has also been found for high redshift ($z \sim 0.5-2$) RQQ, RLQ and FR II radio galaxies with respect to their local counterparts (e.g. McLure & Dunlop 2000; Kukula et al. 2001). It seems that there is basically no size-evolution of the host galaxies of QSOs and radio galaxies independent of radio-power at least up to redshifts of 1, perhaps even up to redshifts of 2.

5.2. Evolution?

As we have shown in the previous subsection, we found evidence for luminosity evolution of the host galaxies of our

Table 4. Evolutionary + K-corrections to the I-band values.

Object	m_I	$R-I$	K+e(I)	μ_R	M_R
PKS 0057–338	19.60	1.33	0.97	18.24	−24.47
PKS 0406+121	19.91	1.04	0.38	19.76	−23.41
PKS 0754+100	17.76	0.72	0.15	22.61	−23.00
PKS 0820+225	20.67	1.27	1.16	20.50	−23.93
RX J0930.9+3933	18.92	1.27	0.51	21.78	−23.87
TXS 1040+224	18.60	1.14	0.44	20.21	−23.93
1207+39W4	18.92	1.24	0.49	23.16	−23.81
Q 1214+1753	18.99	1.32	0.57	21.05	−24.01
RX J1422.6+5801	18.86	1.27	0.51	22.62	−23.92
TXS 1428+370	18.91	1.14	0.44	18.94	−23.60
OV −236	18.31	0.84	0.20	21.81	−23.32
B2 0937+26	19.51	1.03	0.38	21.33	–22.81
MS 2347.4+1924	18.95	1.06	0.39	19.41	–23.75

high-z BL Lacs with respect to local samples, whereas the half-light radii seem to be constant over a large redshift range. To constrain the possible luminosity evolution further, we applied the evolutionary models of Maraston (1998) and Maraston & Thomas (2000) to our data and converted them to Cousins R-band. We assumed a formation of an elliptical galaxy at $z = 2$ (13 Gyrs ago in our cosmology) with passive evolution thereafter. The results for the core sample and the two objects without core are tabulated in Table 4.

The median absolute R-band magnitude of our evolutionary corrected core sample is now $\langle -23.9 \rangle \pm 0.4$, which is in perfect agreement with the results obtained for lower-redshift BL Lac samples (which are only K-corrected, but where the evolutionary correction is mostly relatively small). A comparison is shown in Table 5.

To investigate the properties of our host galaxies even further, we use the projection of the Fundamental Plane for elliptical galaxies, the so-called Kormendy relation (Kormendy 1977), which relates the half-light radii (r_e) and the surface brightness at that radius (μ_e).

Our best linear fit to the core sample using the values from Table 3 for the Kormendy-relation is $\mu_e = (14.7 \pm 0.7) + (5.3 \pm 0.7)\log(r_e)$. As discussed in Abraham et al. (1992) and Dunlop et al. (2003) a slope of ∼5 indicates that the galaxy scalelengths have not properly been constrained (the modeling procedure was not able to break the $\mu_e - r_e$ degeneracy). Since we have observed strongly core-dominated objects at high redshift from ground, it can not be ruled out that this effects our r_e-measurements. However, one should always bear in mind that we are dealing with a small sample and that evolutionary effects have not been taken into account here. In fact, 8 out of 11 objects very nicely follow a narrow relation. The three which deviate strongly are PKS 0058–338 and OV –236 (whose host galaxy brightness is probably under/overestimated, see Appendix A) and PKS 0754+100 (the source with the smallest redshift in our sample). If we restrict our analysis to the 8 sources following the narrow correlation our best fit would be $\mu_e = (15.4 \pm 0.4) + (4.4 \pm 0.4)\log(r_e)$. Now the slope is much shallower and is similar to the correlations found by FK99 in the R-band ($\mu_e = 16.5 + 4.6\log(r_e)$), by Cheung et al. (2003) in the K-band ($\mu_e = 14.2 + 4.6\log(r_e)$) and is comparable to the HST-results by U00 within the errors ($\mu_e = (17.2 \pm 0.7) + (3.9 \pm 0.9)\log(r_e)$).

Table 5. Comparison to other studies.

Sample	N (Obj)	$\langle z \rangle$	$\langle M_R \rangle$ [mag]	$\langle r_e \rangle$ [kpc]
Present study	11	0.6	-23.9 ± 0.4	10.5 ± 7.0
CFHT (W96)[a]	43	0.3	-24.0 ± 0.7	12.2 ± 9.9
XBL-NOT (FK99)	45	0.3	-23.9 ± 0.6	8.9 ± 4.8
HST-Snap (S00)	64	0.3	-23.7 ± 0.6	8.5 ± 5.6
RBL-NOT (P02)	11	0.2	-23.8 ± 0.6	14.8 ± 8.7
RGB-NOT (N03)	62	0.2	-23.8 ± 0.8	13.2 ± 0.8

[a] $r - R = 0.3$ assumed, r_e converted from $q_0 = 0.5$ to $q_0 = 0$. All other studies tabulate Cousins R values and use $H_0 = 50$, $q_0 = 0$.

For a more reliable treatment of the Kormendy relation we proceeded as follows. For the 149 measurements of FK99, U00 and N03 (40, 60 and 49, respectively) we calculated μ_e from their tabulated m_R and r_e values corrected for extinction using the data from NED (as for our sample), for cosmological dimming and K-correction and evolution using the evolutionary models of Maraston (1998) and Maraston & Thomas (2000). Note, that the μ_e values given in Table 2 of U00 were erroneously not corrected for extinction; the extinction correction was applied, however, for their Fig. 6 (Scarpa, priv. com.).

For our sample we used the values corrected for evolution from Table 4. The resulting diagram is shown in Fig. 4. Obviously, all the objects of our core sample (and even the two objects without a core) fall nicely into the region occupied by the measurements of FK99, U00 and N03. The best linear fit through our data gives now $\mu_e = (16.0 \pm 0.4) + (5.2 \pm 0.4)\log(r_e)$ compared to $\mu_e = (17.3 \pm 0.2) + (3.9 \pm 0.2)\log(r_e)$ for the combined FK99, U00 and N03 sample. Irrespective of the evolutionary correction, the slope for our sample remains the same, albeit somewhat smaller scatter. Again, the small number statistics makes the fit very uncertain. For example, the object, which deviates from the Kormendy relation at $\log(r_e) \sim 1.1$, $\mu_e \sim 22.7$ mostly is PKS 0754+100. The properties of its host galaxy were also derived by Falomo (1996) and N03 in R-band. If we use their m_R and r_e values, and apply the same corrections as we have done for Fig. 4, we would derive $\log(r_e)/\mu_e = 1.1/22.7$ and $0.85/21.1$ for Falomo (1996) and N03, respectively. Their and our measurement all lie about 1 mag below the Kormendy-relation. By removing this object and the two with uncertain photometry (PKS 0057–338, OV −236), the slope of the Kormendy relation would again be in the range determined in other studies. To prove, if the slope still remains relatively steep or becomes shallower, requires another set of at least a dozen sources at $z > 0.5$. In addition, our luminosity bias affects the fit. It is very hard to detect and resolve faint host galaxies with small half-light radii from ground. The HST with its new wide-field imager is certainly an attractive alternative.

It is interesting to compare the results obtained for BL Lac hosts at $z > 0.5$ by FK99, U00 and N03 to ours. 13 out of their 149 measurements used here have been taken for

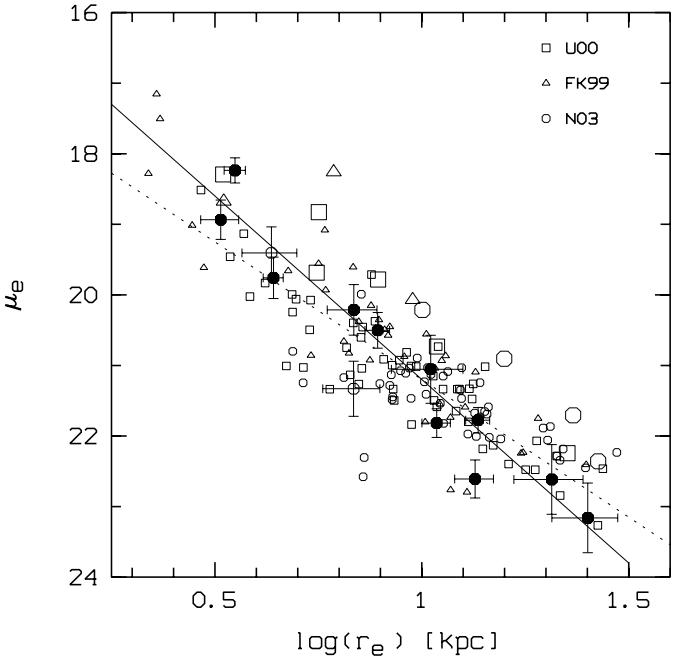

Fig. 4. Kormendy relation for our core sample (black dots) and the two objects without a core (open circles) compared to observations of FK99, U00 and N03. The literature measurements for $z > 0.5$ sources have been coded with larger symbols. All data have been homogeneously corrected for extinction using the values from NED, cosmological dimming and for K-correction and evolution using the models of Maraston (1998) and Maraston & Thomas (2000). In addition our measurements have been converted to the *R*-filter. The solid line gives the best fit to our data, whereas the dashed line show the best fit to the combined FK99, U00 and N03 sample. Note that the measurements of $z > 0.5$ sources from the literature are offset (brighter at a given r_e) with respect to the remaining sources. See text for details.

8 $z > 0.5$ BL Lacs. Four of them are observed within at least two different studies with differences of $\Delta m_R = 0.2-1.4$ mag. Using the evolutionary corrected values we obtain $M_R = \langle -24.8 \rangle \pm 0.5$ for these 13 measurements compared to $M_R = \langle -23.7 \rangle \pm 0.6$ for their 136 measurements of $z < 0.5$ BL Lac hosts. The median value for the $z > 0.5$ hosts in the combined sample is about 1 mag brighter than the ones obtained in the present study. This illustrates that a luminosity bias is also present in the combined sample, which can also be seen in Fig. 4.

In our and the combined sample of FK99, U00 and N03, there are clear indications that BL Lac hosts at $z > 0.5$ are more luminous but have similar half-light radii with respect to their low-redshift counterparts. The BL Lac hosts up to redshifts of one all follow well the Kormendy-relation. As we have shown their properties are consistent with being passively evolving galaxies formed at least 13 Gyrs ago (at $z \sim 2$ on our cosmology). Their properties are also very similar to the ones obtained for RQQ, RLQ and radio galaxies up to redshifts of at least 1. Thus it seems that the host galaxy does not know, whether it harbors a radio quiet or a low-power or high-power radio-loud AGN.

5.3. Future prospects

Within the "Grand Unification" hypothesis (Urry 2003) AGN activity represents a particular phase of normal galaxy evolution. There is growing evidence from morphological and kinematical measurements for low-z AGN, that their hosts are indeed indistinguishable from normal (luminous) elliptical galaxies. At higher-redshift, the imaging data for RQQ and high-luminosity radio-loud AGN (RLQ/FR IIs) also supports the "Grand Unification" hypothesis. Our results indicate that the same is valid for the low-luminosity radio-loud AGN (BL Lacs/FR Is). Unfortunately, we are subject to a luminosity bias, which is hard to overcome.

As already described in the introduction, FR I radio galaxies are hard to find at higher redshifts. Therefore, using BL Lacs instead is the only way out to study host galaxy evolution at higher redshifts for these type of AGN. Only 50% out of the ~880 BL Lacs known have a measured redshift or an upper limit, which is sometimes uncertain (based on one line) or even wrong. The situation is very poor at somewhat higher redshift, only 70 BL Lac objects at $z > 0.5$ from a wide variety of studies are listed in the Véron-catalog. This clearly demonstrates that it is imperative to determine redshifts for a large sample of BL Lac objects. In fact, several groups started to work on that issue (e.g. Carangelo et al. 2003). But how to pick out specifically those presumably at high-z? Although it is still not clear whether low-frequency peaked (mostly RBL) and high-frequency peaked (mostly XBL) BL Lac objects evolve differently or not (e.g. Rector et al. 2000; Rector & Stocke 2001; Beckmann et al. 2003 and references therein), RBL should be preferred, since their spectral energy distribution peaks at optical-NIR wavelengths.

One attractive alternative could be the use of the first well-defined sample of optically-selected BL Lac objects (2QZ) extracted from the 2dF QSO redshift survey (Londish et al. 2002, 2003). It contains ~50 sources and is unbiased with respect to X-ray or radio-flux levels. Using the 2QZ quasar evolution model (Boyle et al. 2000; Croom et al. 2001) a median redshift of $\langle z \rangle = 1.1$ is predicted. This is supported by the first spectroscopic results (Londish et al. 2003). Once, the redshifts are known for the entire 2QZ-sample, a homogeneous very deep high-resolution imaging study (preferably in the NIR) of the 2QZ-sample could shed new light on the evolution of BL Lac host galaxies up to redshifts of ~1.5.

6. Summary

We have presented and discussed deep, high-resolution *I*-band images of 24 BL Lac objects in the redshift range $z = 0.3-1.3$. In 17/24 of our objects, we detected an underlying nebulosity, in 11/17 for the first time. We assigned the underlying nebulosity to the BL Lac host galaxy in 11 cases spanning the redshift range $z = 0.3-1$. While we could not detect a core in two sources, two BL Lacs have intervening galaxies along the line of sight (known for the lensed BL Lac S4 0218+35 previously). The remaining BL Lacs with detected underlying nebulosity have either no redshift or are probably misidentified.

Restricting ourselves to the 11 BL Lacs ($\langle z \rangle = 0.6$), where a core and host galaxy was detected, we find that their host galaxies are about 0.6 mag brighter than their low-redshift ($\langle z \rangle = 0.3$) counterparts ($M_R \sim -24.5$ vs. -23.9) indicative of evolution. Contrary, their half-light radii are similar ($\sim$10 kpc).

To study evolutionary effects, we applied evolutionary synthesis models to the data presented here and to a large comparison sample of low-redshift BL Lac objects from the literature. We could show that the properties of the host galaxies of BL Lac objects up to $z \sim 1$ are compatible with passively evolving elliptical galaxies formed at a redshift of $z \sim 2$ (13 Gyrs ago).

Our results, however, are subject to a luminosity bias and need to be confirmed. If they could be confirmed, the host galaxies of low-luminosity radio-loud AGN (BL Lac/FR I) have very similar properties over a wide redshift range to the hosts of radio-quiet QSOs and high-luminosity radio-loud AGN (radio-loud QSO/FR II). This supports the picture of the "Grand Unification" in which AGN activity is a transient phenomenon in galaxy evolution.

Acknowledgements. We thank the ESO staff at the VLT and NTT and the staff at the NOT for their excellent support during the observations, Claudia Maraston for providing the evolutionary corrections in tabular form and Ulrich Hopp for a careful reading of the manuscript. This work was supported by the Deutsche Forschungsgemeinschaft (SFB 439), the VW foundation and the German Federal Ministry of Science and Technology with ID-Nos. 05 2HD50A, 05 2GO20A and 05 2MU104.

References

Abraham, R. G., Crawford, C. S., & McHardy, I. M. 1991, MNRAS, 252, 482 (A91)
Abraham, R. G., Crawford, C. S., & McHardy, I. M. 1992, ApJ, 401, 474
Bade, N., Beckmann, V., Douglas, N. G., et al. 1998, A&A, 34, 459
Barth, A. J., Ho, L. C., & Sargent, W. L. W. 2003, ApJ, 583, 134
Becker, R. H., White, R. L., & Helfand, D. J. 1995, ApJ, 450, 559
Beckmann, V., Engels, D., Bade, N., & Wucknitz, O. 2003, A&A, 401, 927
Bettoni, D., Falomo, R., Fasano, G., et al. 2001, A&A, 380, 471
Bettoni, D., Falomo, R., Fasano, G., & Govoni, F. 2003, A&A, 399, 869
Boyle, B. J., Shanks, T., & Croom, S. M., et al. 2000, MNRAS, 317, 1014
Browne, I. W. A., Patnaik, A. R., Walsh, D., & Wilkinson, P. N. 1993, MNRAS, 263, L32
Carangelo, N., Falomo, R., Kotilainen, J., & Ulrich, M.-H. 2003, A&A, 412, 651
Cheung, C. C., Urry, C. M., Scarpa, R., & Giavalisco, M. 2003, ApJ, 599, 155
Croom, S. M., Smith, R. J., Boyle, B. J., et al. 2001, MNRAS, 322, L29
Dressler, A., Lynden-Bell, D., & Burstein, D., et al. 1987, ApJ, 313, 42
Djorgovski, S., & Davies, M. 1987, ApJ, 313, 59
Dunlop, J. S., McLure, R. J., Kukula, M. J., et al. 2003, MNRAS, 340, 1095
Drinkwater, M. J., Webster, R. L., Francis, P. J., et al. 1997, MNRAS, 284, 85
Falomo, R. 1996, MNRAS, 283, 241
Falomo, R. & Kotilainen, J. 1999, A&A, 352, 85 (FK99)
Falomo, R., Kotilainen, J., & Treves, A. 2001, ApJ, 547, 124
Falomo, R., Carangelo, N., & Treves, A. 2003, MNRAS, 343, 505
Ferrarese, L., & Merritt, D. 2000, ApJ, 539, L9
Floyd, D. J. E., Kukula, M. J., Dunlop, J. S., et al. 2004, MNRAS, in press
Fukugita, M., Shimasaku, K., & Ichikawa, T. 1995, PASP, 945, 1995
Gebhardt, K., Bender, R., & Bower, R., et al. 2000, ApJ, 539, L13
Giavalisco, M. 2002, ARA&A, 40, 579
Govoni, F., Falomo, R., Fasano, G., & Scarpa, R. 2000, A&A, 353, 507
Hamabe, M., & Kormendy, J. 1987, Correlations between $r^{1/4}$-law parameters for bulges and elliptical galaxies. In Structure and Dynamics of Elliptical Galaxies, ed. T. de Zeeuw (Dordrecht: Reidel), IAU Symp., 127, 379
Hawkins, M. R. S., Véron, P., Hunstaed, R. W., & Burgess, A. M. 1991, A&A, 248, 421
Heidt, J., Nilsson, K., Sillanpää, A., Takalo, L. O., & Pursimo, T. 1999a, A&A, 341, 683
Heidt, J. 1999b, Host galaxies and environment of BL Lac objects, in Proc. BL Lac Phenomenon, ed. L. O. Takalo, & A. Sillanpää PASP, 159, 367
Heidt, J., Nilsson, K., Appenzeller, I. et al. 1999c, A&A, 352, L11
Heidt, J., Appenzeller, I., Gabasch, A., et al. 2003a, A&A, 398, 49
Heidt, J., Jäger, K., Nilsson, K., et al. 2003b, A&A, 406, 565
Hewett, P. C., Foltz, C. B., & Chaffee, F. H. 1995, AJ, 109, 1498
Hook, I. M., McMahon, R. G., Irwin, M. J., & Hazard, C. 1996, MNRAS, 282, 1274
Hutchings, J. B. 1995, AJ, 110, 994
Kollgaard, R. I., Laurent-Muehleisen, S. A., Feigelson, E. D., & Palma, C. 1995, ApJ, 449, 61
Kormendy, J. 1977, ApJ, 218, 333
Kormendy, J. 2003, The stellar dynamical search for supermassive Black Holes in galactic nuclei, in Carnegie Observatories Astrophys. Ser. 1, Coevolution of Black Holes and Galaxies, ed. L. Ho (Pasadena: Carnegie observatories, `http://www.ociw.edu/ociw/symposia/series/symposium1/proceedings.html`
Kotilainen, J., Falomo, R., & Scarpa, R. 1998, 336, 479
Kukula, M. J., Dunlop, J. S., McLure, R. J., et al. 2001, MNRAS, 326, 1533
Landolt, A. U. 1992, AJ, 104, 340
Lawrence, C. R. 1996, Observations of lens systems with Keck I, in Astrophysical applications of gravitational lensing, ed. C. S. Kochanek, & J. N. Hewitt (Kluwer), IAU Symp., 173, 299
Lehár, J., Falco, E. E., Kochanek, C. S. et al. 2000, ApJ, 536, 584
Londish, D., Croom, S. M., Boyle, B. J., et al. 2002, MNRAS, 334, 941
Londish, D., Croom, S. M., Boyle, B. J., & Sadler, E. M. 2003, A optically selected sample of BL Lac objects, in Maps of the Cosmos, ed. M. Colless, L. Staveley-Smith, IAU Symp., 216, ASP Conf. Ser., in press
Lowenthal, J. D., Heckman, T. M., Lehnert, M. D., et al. 1995, ApJ, 439, 588
Maglioccheti, M., Maddox, S. J., Wall, J. V., Benn, C. R., & Cotter, G. 2000, MNRAS, 318, 1047
Maglioccheti, M., Celotti, A., & Danese, L. 2002, MNRAS, 329, 377
Magorrian, J., Tremaine, S., Richstone, D., et al. 1998, AJ, 115, 2285
Maraston, C. 1998, MNRAS, 300, 872
Maraston, C. & Thomas, D. 2000, ApJ, 541, 126
McLure, R. J., & Dunlop, J. S. 2000, MNRAS, 317, 249
McLure, R. J., & Dunlop, J. S. 2002, MNRAS, 331, 795

Moran, E. C., Helfand, D. J., Becker, R. H., & White, R. L. 1996, ApJ, 461, 127
Morganti, R., Tadhunter, C. N., Fosbury, R. A. E., et al. 1995, PASA, 12, 3
Nass, P., Bade, N., Kollgaard, R. I., et al. 1996, A&A, 309, 419
Nilsson, K., Pursimo, T., Heidt, J. et al. 2003, A&A, 400, 95 (N03)
Ostriker, J. P., & Vietri, M. 1985, Nature, 318, 446
Oke, J. B. 1990, AJ, 99, 1621
Pagani, C., Falomo, R., & Treves, A. 2003, ApJ, 596, 830
Patnaik, A. R., Browne, I. W. A., King, L. J., et al. 1993, MNRAS, 261, 435
Perlman, E. S., Stocke, J. T., Schachter, J. F., et al. 1996, ApJS, 104, 251
Perlman, E., Padovani, P., Giommi, P., et al. 1998, AJ, 115, 1253
Pesce, J. E., Falomo, R., & Treves, A. 1995, AJ, 110, 1554
Pursimo, T., Nilsson, K., Takalo, L. O., et al. 2002, A&A, 381, 810 (P02)
Rector, T. A., Stocke, J. T., Perlman, E. S., Morris, S. L., & Gioia, I. M. 2000, AJ, 120, 1626
Rector, T. A., & Stocke, J. T. 2001, AJ, 122, 565
Scarpa, R. & Falomo, R. 1997, A&A, 325, 109
Scarpa, R., Urry, C. M., Falomo, R., et al. 1999, ApJ, 521, 134
Scarpa, R., Urry, C. M., Falomo, R., Pesce, J. E., & Treves, A. 2000a, ApJ, 532, 740 (S00)
Scarpa, R., Urry, C. M., Padovani, P., Calzetti, D., & O'Dowd, M. 2000b, ApJ, 544, 258
Stickel, M., Fried, J., & Kühr, H. 1993, A&AS, 98, 393 (S93)
Stickel, M., & Kühr, H. 1993, A&AS, 100, 395
Steidel, C., Dickinson, M., & Persson, S. E. 1994, ApJ, 437, L75
Stocke, J. T., & Rector, T. A. 1997, ApJ, 489, L17
Tinney, C. G. 1999, MNRAS, 303, 565
Urry, C. M. & Padovani, P. 1995, PASP, 107, 803
Urry, C. M., Falomo, R., Scarpa, R., et al. 1999, ApJ, 512, 88
Urry, C. M., Scarpa, R., O'Dowd, M., et al. 2000, ApJ, 532, 816 (U00)
Urry, C. M. 2003, The AGN paradigm for radio-loud objects, in Active galactic nuclei: from central engine to host galaxy, ed. S. Collin, F. Combes, & I. Shlosman, ASP Conf. Ser., 290, 3
Véron, P. 1995, A&A, 310, 381
Véron-Cetty, M. P., & Véron P. 2003, A&A, 412, 399
Wall, J. V., & Peacock, J. A. 1985, MNRAS, 216, 175
White, R. L., Becker, R. H., Gregg, M. D., et al. 2000, ApJS, 126, 133
Wilkinson, P. N., Browne, I. W. A., Patnaik, A. R., Wrobel, J. M., & Sorathia, B. 1998, MNRAS, 300, 790
Wright, S. C., McHardy, I. M., Abraham, R. G., & Crawford, C. S. 1998, MNRAS, 296, 961
Wolf, C., Wisotzki, L., Borch, A., et al. 2003, A&A, 408, 499
Wurtz, R., Stocke, J. T., & Yee, H. K. C. 1996, ApJS, 103, 109 (W96)
Zirm, A. W., Dickinson, M., & Dey, A. 2003, ApJ, 585, 90

Online Material

Appendix A: Notes on individual objects

The numbers given in this section, refer always to the fit with core + de Vaucouleurs model and ϵ = PA = 0 unless otherwise noted.

PKS 0057–338: this BL Lac lies behind the Sculptor dSph galaxy (Tinney 1999). The analysis was hampered by the presence of a 20 mag galaxy ∼2.″3 to the W (which was fitted away recursively) and the presence of an elongated object (either a faint disturbed galaxy behind Sculptor or two overlapping Sculptor stars) ∼1.″2 to the NE. The host galaxy is clearly resolved and is relatively bright ($M_I = -26.04$) and compact (r_e = 3.54 kpc). Due to the extreme crowding the host galaxy luminosity could be overestimated.

S4 0218+35: this source is the only BL Lac, which is known to be lensed. It consists of two images of a compact flat-spectrum radio source at z = 0.96 (Lawrence 1996) separated by 335 mas and possesses an Einstein ring of the associated radio jet (Patnaik et al. 1993). The lensing galaxy has a redshift of z = 0.685 (Browne et al. 1993). Based on HST observations Lehár et al. (2000) found the lensing galaxy to be most likely a late-type galaxy with m_I = 20.06 and r_e = 0.″19 (using a circular galaxy). For the two BL Lac images A and B they give m_I = 21.8 and 19.39 respectively.

According to our fits, a disk model is preferred over an elliptical model ($\chi^2_{\rm bulge} = 1.32, \chi^2_{\rm disk} = 1.11$) with ϵ = 0.1 and PA = 85°. The brightness we derived for the lensing galaxy (m_I = 20.03) is in excellent agreement with Lehár et al. (2000). Our half-light radii differ by more than a factor of 2 (0.″49 vs. 0.″19), but this may be due to the fact that at z = 0.685 Hβ and [O III] fall into the wavelength range covered by our I-filter, whereas the half-light radii given in Lehár are obtained from fits to their H-band image of S4 0218+35. For the BL Lac component B we found m_I = 19.33. The BL Lac component A (masked out for the fits) is apparent on the model-subtracted image, but we could not obtain an useful measurement of its brightness (see Fig. 2).

Q 0230+3429: this source was classified as a BL Lac at z = 0.458 by Moran et al. (1996), who neither show a spectrum nor give line identifications. Hook et al. (1996) give z = 0.50 based on a clear detection of narrow [O II] and [O III] emission lines. Our NOT-image of this source (Fig. 2) shows two objects, one extended and one compact, separated by 1.″2. To determine, which of the two objects is the BL Lac, we selected 16 non-saturated stars from the APM catalog. To these we fitted an astrometric solution taking into account the zero point and rotation of the field, but not higher order terms. The rms scatter of the residuals is 0.″35 in α and 0.″18 in δ. By using the radio coordinates from Wilkinson et al. (1998), which have an accuracy of 55 mas, we determined the pixel position of the radio source. This position is coincident with the extended object (see Fig. 2).

For the extended object, a fit with a pure bulge was almost equally good as the fit with core+bulge ($\chi^2_{\rm b} = 1.17, \chi^2_{\rm b+c} = 1.16$). If a core is present, it is about 5 mag weaker than the host galaxy. At z = 0.5 (or 0.458), the host galaxy would be extremely luminous ($M_I = -27.85$) and huge (r_e = 39.65 kpc). For z = 0.08, we would derive r_e = 10 kpc and $M_I = -23.2$ for this galaxy, which is more reasonable. The compact object 1.″2 NW of the extended object is unresolved and has m_I = 18.10.

There are several possibilities to resolve this ambiguity. Either the radio source is not a BL Lac and/or the unresolved object 1.″2 to the NW is an AGN or the (faint) BL Lac is seen through (or located in) a nearby, large and bright galaxy (and thus a microlensing candidate in the former case).

Moran et al. (1996) detected several passive elliptical galaxies with 6 cm fluxes of up to a few 100 mJy in the EMSS 2σ catalog. This may be a further case here. If the unresolved object is an AGN at $z \sim 0.5$, it would have roughly $M_I = -24.9$, reasonable for a QSO. The offset between the radio position and the optical position from POSS in Hook et al. (1996) is about 1″ (practically on the unresolved object). Therefore it is possible that the unresolved source is a QSO at z = 0.5, whereas the nature of Q 0230+3429 is unclear.

PKS 0406+121: the host galaxy of this BL Lac is clearly resolved, but no galaxy type preferred. For an elliptical host we find m_I = 20.25, r_e = 0.″54. The redshift (z = 1.02) based on a weak emission line at 7528 Å given by Kollgaard et al. (1995) is most likely wrong. At this redshift the host would be extremely luminous ($M_I = -27.7$). In our VLT spectrum we detected the line at 7528 Å as well, but in addition very weak emission lines at 5605 Å (partly blended with the strong night sky emission line at 5577 Å) and 7311 Å (Fig. A.1). By identifying these lines with [O II] , Hβ and [O III], we derive z = 0.504 for the BL Lac. Its host galaxy has now $M_I = -24.5$ well in the range found for the rest of our sample.

PKS 0426–380: contrary to S93 and S00 we detected a galaxy in this object. Our model fits prefer a disk over an elliptical galaxy with m_I = 20.4 and r_e = 0.″7. Our spectrum shows, in addition to the Mg II absorption at z = 1.03 found by S93, another Mg II absorption at z = 0.559 (4362 Å). This absorption line is already visible in the spectrum presented by S93 (see their Fig. 2). Furthermore, a broad emission line at 5906 Å is apparent, which we identify with Mg II at z = 1.111 confirming now a further BL Lac at $z > 1$ in the 1 Jy sample of BL Lac objects (see Fig. A.1). Since the galaxy detected in this object has the largest decentering according to our fits (0.″17) and since an elliptical galaxy at z = 1.111 with m_I = 20.4 would be extremely luminous ($M_I = -26.65$), we believe that we have detected the absorbing galaxy at z = 0.559. This galaxy has similar properties to the ones found for absorbing systems by Steidel et al. (1994). There is a faint galaxy ($m_I \sim 23.2$) 4″ NE of the BL Lac. S00 noted a very small companion galaxy at 0.″51 from the BL Lac. Either of those galaxies could be responsible for the absorption at z = 1.03. PKS 0426–380 is a clear microlensing candidate.

PKS 0754+100: the host galaxy is resolved with $M_I = -23.8$ and r_e = 13.5 kpc. Falomo (1996) and N03 could resolve the host galaxy in the R-band as well. Their results are similar to the one obtained here (when converted from I to R). The host galaxy was not resolved by Wright et al. (1998) in the NIR and S00 in the optical, A91 could resolve the host, but did not give parameters. Note that the widely cited redshift (z = 0.66) of PKS 0754+100 is wrong. Recently, Carangelo et al. (2003) obtained z = 0.266 based on the detection of [O II] and [O III] in the spectrum of PKS 0754+100.

PKS 0820+225: this is the BL Lac with the highest redshift, in which we could detect the host galaxy (z = 0.951). No host galaxy type is preferred. For an elliptical galaxy we derive $M_I = -25.5$ and r_e = 7.9 kpc. Previous attempts to resolve the host galaxy failed (S93, S00, P02).

PKS 0823+033: the analysis of this object was severely hindered by a star of similar brightness 2″ to the E. We could not resolve the host galaxy similarly to S00 and P02. S93 found the BL Lac to be spatially resolved, W96 could possibly detect the host galaxy with $M_R = -23.9$.

RX J0930.9+3933: The host galaxy is large and luminous ($M_I = -25.3$, r_e = 13.8 kpc).

B2 0937+26: a (weak) core was only detected for the disk+core fit. For an elliptical galaxy we found $M_I = -23.91$ and r_e = 6.8 kpc. The results given in Table 3 are derived for ϵ = 0.28, PA = 30°. To make the r_e derived for B2 0937+26 comparable to the ones derived for the ϵ = 0 fits to the other sources, we multiplied r_e by $\sqrt{(1-\epsilon)}$. Note that the redshift for B2 0937+26 given in Perlman et al. (1998) is tentative. It is based on two absorption lines at 5890 Å and at 5945 Å, which are identified with Ca K+H at z = 0.498 (Perlman, priv. com.). While the parameters derived from our fitting procedure are consistent with an elliptical galaxy at a redshift z = 0.498, the absence of a core

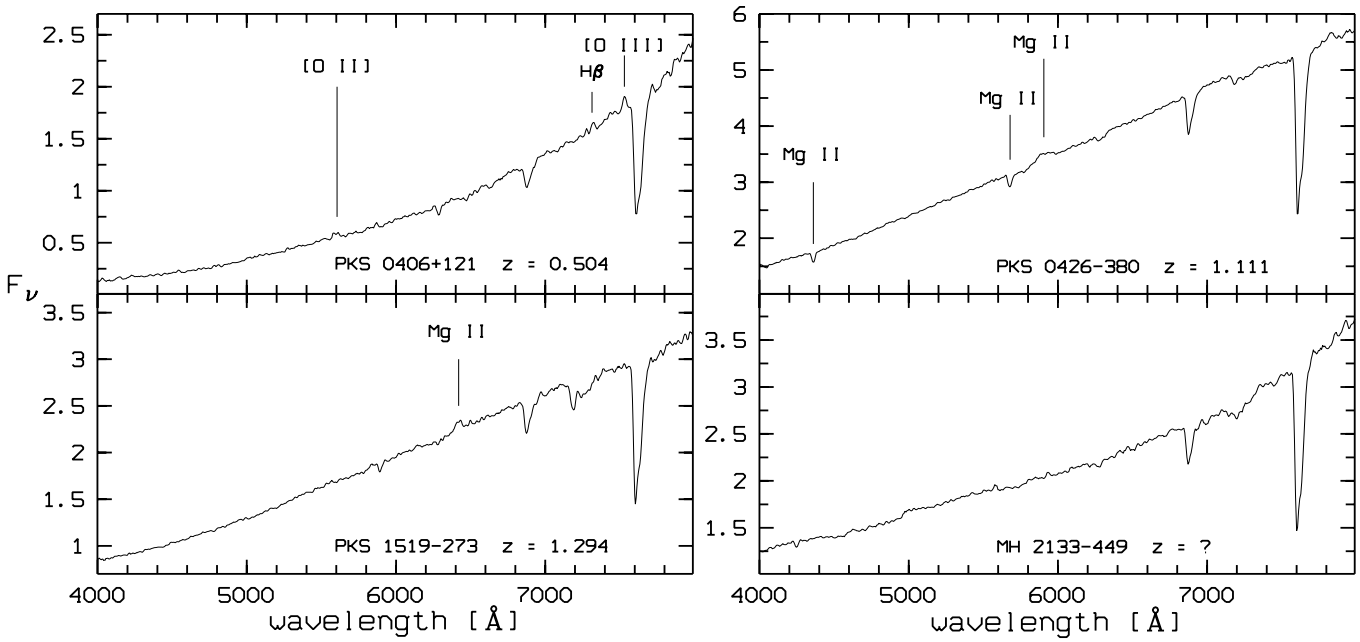

Fig. A.1. Spectra of the four BL Lac objects obtained with the VLT. See Appendix A for details.

implies either a misidentification or a very weak state of the BL Lac during our observations.

TXS 1040+224: the host galaxy is clearly resolved with $M_I = -25.15$ and $r_e = 6.9$ kpc. An elliptical host is preferred.

1207+39W4: the host galaxy is well resolved, luminous and large ($M_I = -25.15$, $r_e = 25.5$ kpc). U00 found $M_R = -24.4$, which is in good agreement with our measurement (assuming $R - I = 0.7$, Fukugita et al. 1995). The host galaxy was also resolved by W96. Our r_e (2.″8) is larger than the ones reported by S00 and W96 in R-band (1.″2 and 2.″2, respectively).

Q 1214+1753: the host galaxy is resolved, but no galaxy type preferred. For an elliptical host we derive $M_I = -25.5$ and $r_e = 10.5$ kpc.

1ES 1249+174E: similarly to S00 the host galaxy was not resolved.

PKS 1349–439: we could not detect the host galaxy of this low galactic latitude ($b = 18°$) BL Lac with unknown redshift. There is a Sy I galaxy ∼57″ SE of PKS 1349–439 at $z = 0.052$ (Véron 1995).

RX J1422.6+5801: the host galaxy was easily resolved and is large ($r_e = 21$ kpc) and luminous ($M_I = -25.33$). No galaxy type is preferred. S00 failed to resolve the host galaxy.

TXS 1428+370: we found a typically bright ($M_I = -24.8$), but relatively small ($r_e = 3.3$ kpc) host galaxy, with an elliptical host slightly preferred.

PKS 1519–273: the analysis was seriously hampered by the presence of a star 0.″8 E of the BL Lac. S93, S00 and we could not detect the host galaxy. Using our VLT spectrum, we could derive a redshift for PKS 151–273 (Fig. A.1). A broad emission line at 6419 Å is present, which we identify with Mg II at $z = 1.294$ making this object the BL Lac with the highest confirmed redshift in the 1 Jy sample of BL Lac objects. The spectrum of the nearby star (parts of its light came into the slit) shows it to be a K star.

OV −236: scattered light from a 6th magnitude star (HD 182286) ∼5′ SE of this low galactic latitude ($b = -20°$) BL Lac had to be removed before the analysis. The host galaxy of one of our nearest BL Lac objects in our sample ($z = 0.352$) is nicely resolved. Our results are comparable to the one obtained in the R band by W96 (once corrected for the different filters used), who could marginally resolve the host galaxy. This source was observed with the VLT during periods of non-photometric observing conditions on the night Aug, 13/14 1999 (partly thick cirrus). Therefore the brightness of the host galaxy is most likely underestimated.

PKS 2029+121: our analysis of this high-redshift BL Lac ($z = 1.215$) was seriously hampered by a K star (Stickel & Kühr 1993) of similar brightness 2.″5 to the E. PKS 2029+121 is unresolved. Several faint objects within a few arcsec close to PKS 2029+121 can be seen. These may cause the absorption lines at $z = 1.115$ found by Stickel & Kühr (1993) and Stocke & Rector (1997) in the spectrum of this BL Lac.

PKS 2131–021: this high-redshift ($z = 1.285$) BL Lac remains unresolved as in the studies by S93, S00 and P02.

MH 2133–449: the redshift of this BL Lac is not known. We were able to marginally resolve the host galaxy ($m_R = 21.3$, $r_e = 3.″7$) on our R band image taken at the VLT. Assuming $z = 0.7$ we would derive a reasonable brightness ($M_R = -24.0$) albeit with a large host galaxy ($r_e = 36$ kpc). Our VLT spectrum (Fig. A.1) is featureless as in Hawkins et al. (1991).

PKS 2240–260: this BL Lac was unresolved in the studies by S93, S00, P02 and Cheung et al. (2003) as in our study.

MS 2347.4+1924: contrary to FK99 we could not detect a core for a bulge+core model. In addition, for a fit of an elliptical galaxy with $\epsilon = 0$, we could not obtain a satisfactory fit. The results given in Table 3 are derived for $\epsilon = 0.44$, PA = 65°. To make the r_e derived for MS 2347.4+1924 comparable to the ones derived for the $\epsilon = 0$ fits to the other sources, we multiplied r_e by $\sqrt{(1-\epsilon)}$. The according values ($M_I = -24.9$, $r_e = 4.4$ kpc) are in good agreement to those obtained by FK99 from R-band imaging ($M_R = -23.7$, $r_e = 3.3$ kpc). Curiously, a somewhat better fit was obtained for a disk+core model. For comparison, we show in Fig. 1 the radial profile for the fit with pure bulge and the fit with core+disk. The absence of a core implies either a misidentification or a very weak state of the BL Lac during our observations (with $m_R = 21.9$, the core of MS 2347.4+1924 was already very faint during the FK99 observations).